ELSEVIER

Sedimentary Geology 117 (1998) 11–32

Sedimentary Geology

Architectural stacking patterns of the Ebro delta controlled by Holocene high-frequency eustatic fluctuations, delta-lobe switching and subsidence processes

L. Somoza [a,*], A. Barnolas [a], A. Arasa [b], A. Maestro [a], J.G. Rees [c], F.J. Hernandez-Molina [d]

[a] *Marine Geology Division, ITGE, Geological Survey of Spain, Ríos Rosas 23, 28003 Madrid, Spain*
[b] *Departament Geologia Dinàmica, Geofísica i P. Universitat de Barcelona, Campus de Pedralbes, 08071 Barcelona, Spain*
[c] *Coastal and Engineering Geology Group, British Geological Survey, Kingsley Dunham Centre, Keyworth, Nottingham NG12 5GG, UK*
[d] *Facultad Ciencias del Mar, Universidad de Cádiz, Rio San Pedro s/n. 11510 Puerto Real, Cadiz, Spain*

Received 15 January 1997; accepted 10 November 1997

Abstract

During the Late Pleistocene and Holocene (125 ka B.P. to present) a Type 1, 4th-order, depositional sequence, comprising regressive, lowstand, transgressive and highstand system tracts, formed worldwide. The Holocene (10 ka B.P. to present) part of this contains the latest and present highstand systems tract (HST). Within this and the underlying transgressive systems tract (TST) of the Ebro delta, in northeastern Spain, higher-frequency, 5th- to 6th-order, sea-level fluctuations are recognised. These form retrogradational and progradational high-frequency depositional sequence sets within the TST and HST, respectively. Each high-frequency sequence comprises: (1) a basal, highly reflective, shell lag, associated with an erosional (transgressive) surface; (2) aggradational deposits which seawards consist of a wedge of marine clays with transparent seismic facies, but inland are represented by thick peats; (3) progradational deposits, composed of sandy delta-front facies, displaying slope clinoforms; these pass seawards into prodeltaic grey silts, and landwards, into red silts and pebbly sands of delta-plain facies. The progradational deposits downlap towards their bases. The aggradational deposits formed in response to a period of rising sea-level and a rapid increase in accommodation space. Progradation began when sediment supply to the delta exceeded accommodation space as a result of relative sea-level fall. The relative sea-level curve for the delta has a stepped character, caused by the punctuation of the 4th-order sea-level trend by higher-frequency eustatic fluctuations as well as by high subsidence rates, of about 1.75 mm per year. The TST comprises retrogradational parasequences that onlap the underlying Pleistocene gravels. The maximum flooding surface separating the TST from the HST, was formed about 6900 yrs B.P. on the basis of ^{14}C dating of peats. The HST comprises progradational deltaic and aggradational units, stacked as progradational high-frequency parasequence sets. The HST of the Ebro delta is compared with other deltaic sequences around the world, in particular with that of the Mississippi delta. A tentative chronology of the high-frequency climatic and eustatic oscillations influencing deltaic sedimentation globally over the last 7000 years is presented.

Keywords: Holocene; delta; sea-level changes; high-resolution seismic; sequence stratigraphy; radiocarbon dating; high-frequency cycles; subsidence rates; Mediterranean; Spain

* Corresponding author.

0037-0738/98/$19.00
PII S0037-0738(97)00121-8

1. Introduction

Since the 1940s, studies of the sedimentary architecture of Holocene deltas have related their origin to highstand sea-level stabilisation over the last 7000 years (Shepard et al., 1960; Scruton, 1960). Initial studies determined that they constitute single bodies that were deposited under a range of depositional environments and facies, but are characterized by large-scale sigmoidal internal configurations (Maldonado, 1972; Galloway, 1975; Miall, 1984; Wright, 1985; Kindinger, 1988). Avulsion and channel abandonment processes were considered to be the main delta constructional processes, the resulting deposits subsequently being modified by compaction and growth faulting (Mandl and Crans, 1981; Coleman et al., 1983).

Since the classic paper of Fairbridge (1961), two contrasting Holocene sea-level curves have been used to explain delta evolution and overall coastal depositional architectures. The first suggests an asymptotic decrease in the rate of eustatic sea-level rise through the Holocene, which has given rise to the initiation and development of deltas on a world-wide basis (Stanley and Warne, 1994); a model commonly applied to subsiding lowland areas (Van de Plassche and Roep, 1989; Stapor et al., 1991). However, high-resolution oxygen isotope curves from ice-cores and deep-sea cores show the occurrence of high-frequency climatic pulses, with periodicities of about 11,000, 6100, 2300, 1450 and 512 years, that affect the global ice cover volume and thus create high-frequency sea-level fluctuations (Dansgaard et al., 1989). These suggest that the asymptotic curve is an oversimplification and that a trend curve, punctuated by a number of sea-level stillstands, or minor falls, is more realistic (e.g. Díaz and Maldonado, 1990; Hernandez-Molina et al., 1994; Larcombe et al., 1995).

The application of sequence stratigraphy (Vail et al., 1977; Posamentier et al., 1988) to Late Pleistocene and Holocene shelf and coastal deposits (Thorne and Swift, 1991) has shown that the large-scale architecture of deltas, defined by the geometry of progradation, aggradation and retrogradation, is mainly governed by sediment yield and relative sea-level change (Postma, 1995). Locally, delta construction, or modification, is influenced by rapid subsidence processes, mainly growth faulting and compaction. The avulsion of delta lobes, until recently seen to be a basically random process, is now seen to be caused by superimposed processes such as climate change and sea-level fluctuations (Swift et al., 1991). For instance, the Mississippi delta-lobe switching has recently been related to high-frequency eustatic events during the Holocene highstand (Lowrie and Hamiter, 1995).

Within the present, 4th-order, sea-level cycle that has occurred since the last interglacial (isotope stage 5e), higher-frequency, 5th- and 6th-order cycles (Mitchum and Van Wagoner, 1991; Posamentier and James, 1993) may be recognised. The stratigraphical sequences which result from these, referred to as high-resolution sequences, have been differentiated in coastal and shelf sedimentary sequences by studies of cores and high-resolution seismic reflection surveys. The 5th- and 6th-order eustatic cycles have been used to explain the depositional architecture of many coastal and shelf deposits in the Northern Hemisphere, including: the deltas of the Nile (Stanley and Warne, 1993), Rhône (Gensous and Tesson, 1992; Gensous et al., 1993), Tiber (Belloti et al., 1994), Catalonian coast (Checa et al., 1988; Díaz et al., 1990) and Alboran Sea (Hernandez-Molina et al., 1996) in the Mediterranean; deltas of the Guadalquivir and Guadiana rivers in the Gulf of Cadiz (Somoza et al., 1997), of the 'Galician Rias' (Somoza and Rey, 1993), the Rhine–Meuse (Tornquist, 1994) and Mississippi (Fairbridge, 1988; Boyd et al., 1989; Lowrie and Fairbridge, 1991; Kosters and Suter, 1993;) in the Atlantic; deltas of the Fraser river (Williams and Roberts, 1989), Slave river (Vanderburgh and Smith, 1988) and Yangtze (Stanley and Chen, 1993) in the Pacific; the Tigris–Euphrates–Karun delta (Lambeck, 1996) in the Arabian Gulf and the Krishna delta (Rao et al., 1990) in the Indian Sea.

The aim of this paper is to analyse the architectural stacking patterns of the Holocene depositional units of the Ebro delta (Fig. 1), and interpret them in terms of relative mean sea-level (RMSL) fluctuations. The correlation of these patterns with those of accurately dated Mediterranean beach and spit-bar deposits has allowed evaluation of the range and age of high-frequency sea-level fluctuations.

2. Methods and database

The first geological studies of the Ebro delta were carried out in the 1960s, resulting in detailed topographic and geotechnical maps (Hydrotechnic Corporation, 1966). Hydrocarbon exploration wells drilled during the late 1960s, gave Solé et al. (1961), Macau (1961), Maldonado and Riba (1971) and Maldonado (1972) the opportunity of establishing the Holocene evolution of the delta. Geological background data from petroleum exploration wells and multichannel seismic reflection profiles were published by IGME (1987) and compiled to make the geological sheets of the continental shelf of the Ebro margin (IGME, 1986). Many multidisciplinary studies, dealing with physical water mass properties, oceanic currents, sedimentary processes and Quaternary evolution of the continental shelf of the Ebro delta (Nelson and Maldonado, 1990) have now been undertaken.

The present study of the Holocene sequence stratigraphy and depositional architecture of the delta has made use of the following datasets (Fig. 1):

(1) High-resolution seismics, consisting of two 30-km-long profiles (Geopulse, 350-175 J), along the left and right banks of the Ebro river. These cross the delta-plain from the landward side of the delta to the present delta-front lobe (Fig. 1).

(2) Six boreholes (ITGE 1 to 6) between 20 and 60 m long, drilled for this study on the delta plain and recent delta-front lobes; these have allowed the correlation of the high-resolution seismic facies. Data from four petroleum exploration wells between 500 and 2500 m deep, drilled on the delta plain, published by IGME (1987). Logs of wells drilled for civil engineering purposes and the unpublished work of Arasa (1994). Well logs (previously published) of other boreholes drilled on the delta plain (Macau, 1961; Maldonado, 1972).

(3) Subsurficial electrical-conductivity maps of the delta-plain, made for water exploration (Hydrotechnic Corporation, 1966), have allowed correlation of high-resolution seismic profiles, and facilitated the sub-surface mapping of Holocene delta-front lobes.

(4) Historical documentation of the evolution of delta-front mouths and of the river-channel avulsion over the last 1000 years.

3. Characteristics of the Ebro delta and geological background

The Ebro delta, with an area of 320 km^2 and a volume estimated at 28 km^3, is the third largest delta in the Mediterranean (after those of the Nile and Rhône). The width of the Ebro continental shelf varies from 40 km to the north of the delta to 70 km in the south. The gradient of the prodelta slopes ranges between 0.1° and 0.5° and is less than 0.1° on the outer shelf (Díaz et al., 1990). Rapid changes in the delta coastline have been frequently reported since the 1950s (e.g. Maldonado, 1972, 1975; Guillén and Díaz, 1990; Jiménez and Sánchez-Arcilla, 1993; Serra and Riera, 1993). The active delta lobe has, at times, advanced at rates of up to 60 m per year (e.g. 1890), yet retreated rapidly during other periods for instance in 1950 (Rodriguez-Ortiz et al., 1978) and during the late 1960s when the coastline retreated dramatically by about 3 km, affecting the stability of the active Buda lobe and causing destruction of the Buda lighthouse at its tip. By the early 1940s the lobe was abandoned and a new river mouth was generated (Fig. 1).

The Ebro delta basin consists of an accumulation of between 500 and 2500 m of Plio–Quaternary deposits which unconformably overlie Miocene deposits (IGME, 1986). The basement of the delta consists mostly of Lower Jurassic limestones and dolomites, and Upper Cretaceous marls and bioclastic limestones. These are densely faulted by normal faults with strikes of 70°N (Catalanide Ranges) and 290°N (Iberian Ranges) which bound structural highs and lows parallel to the present coast. The depth of the top of the Mesozoic basement varies considerably, between 214 m in the San Carlos 1 well on the landward side of the delta, to 1595 m in the Amposta well on the present delta front, to 2560 m in the Delta C1 well located on the tip of the present prodelta (Fig. 1). The top of the Miocene beneath the delta is marked by a strong reflector that corresponds to a regional erosional surface (unconformity) which developed during the Mediterranean desiccation (the Messinian salinity crisis). This surface dips steeply basinwards, occurring at 214 m in the San Carlos 1 well, at 1125 m in the Amposta well, and at 1864 m in the Delta C1 well, and demonstrates the variation in Plio–Quaternary subsidence rates in

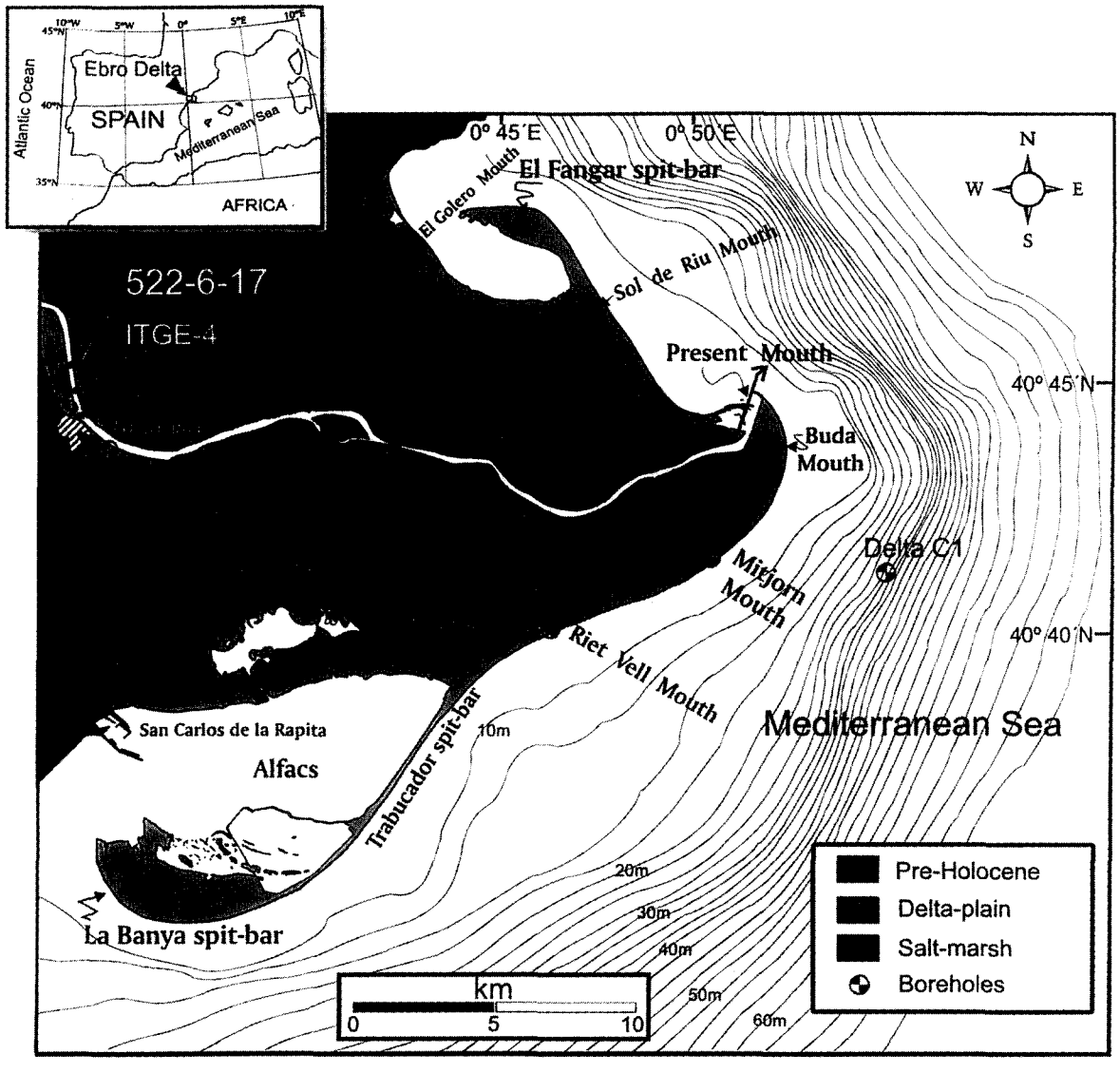

Fig. 1. Map of the Ebro delta showing the bathymetry of the subaqueous prodelta, the location of boreholes and of the high-resolution seismic profile (Fig. 2) along the Ebro. The names of the delta lobes and spit-bar systems referred to in the text are also shown.

the delta area. Above the Messinian unconformity, Miocene strata are overlain by the Plio–Quaternary Ebro Group (Soler et al., 1983) which consists of the Pliocene Lower Ebro Clays that grade upwards and shorewards into the Plio–Pleistocene Ebro Sandstones. The sandstones consist of interbedded shallow-marine conglomerates and marly clays. These downlap onto the underlying Ebro Clays and form a landward-thinning wedge beneath the delta plain.

On the shelf, the Pleistocene deposits comprise thirteen seismic units which show stacked progradational and aggradational reflectors with typical sigmoidal configuration, that are interpreted to have formed in response to Pleistocene glacio-eustatic sea-level changes (Farrán and Maldonado, 1990; Field and Gardner, 1990). The uppermost part of the Ebro Sandstones consists of mid- and Late Pleistocene deposits which overlap all of the underlying deposits

and consist of polygenetic, poorly cemented gravels. They are interbedded with grey plastic clays (identified in oil-wells on the landward margin of the delta, at depths of between 50 and 70 m) which are represented by chaotic and convoluted high-amplitude reflectors on the seismic profiles. Below these, the gravels contain melanges of marly clays and gravels. Along the seismic profiles, the base of the gravel deposits gives rise to a poor reflection, due to limited energy transmission through the gravels; it appears as a discontinuous seaward-dipping reflector between 150 and 180 ms (TWT time). The impedance boundary is correlated with an abrupt lithological change between the gravel and the middle Pleistocene clays (Fig. 2). This surface is marked by an undulating, continuous, strong high-amplitude, seawards-dipping reflector (Maldonado, 1972). Discontinuous reflectors, dipping between 45° and 30° seawards, within the gravels and crossing into the Holocene deposits are interpreted to be growth faults (Crans et al., 1980).

The Holocene deposits of the delta (Fig. 3) have a thickness ranging from 18 m on the landward side of the delta (borehole ITGE 3) to 51 m at the delta front (borehole ITGE 2). The maximum thickness of delta sediments occurs near the mouth of the present Ebro river (Maldonado, 1972); the sediments thin offshore and are absent beyond the middle of the shelf. ^{14}C ages (Díaz et al., 1990) indicate that deposition of the prodelta on the shelf began between about 10,000 and 11,000 yrs B.P.

4. Sedimentary architecture of the Ebro deltaic deposits

The lithology, seismic facies and geometry of the delta deposits have been identified on the basis of correlation between seismic profiles (Fig. 2) and well-logs (Fig. 3). The sedimentary units have been distinguished on the basis of lithology, stratigraphical configuration and geometrical relationship. For the purpose of sequence stratigraphical analysis, the units are divided into progradational (d units) and aggradational (a units) deposits (see below, Fig. 3).

4.1. Progradational deltaic deposits

Progradational units are mainly composed of bioclastic sands, proved in borehole ITGE-6, that pass seawards into fine sands, grey silts and silty clays. Landwards they consist of coarse red sands with isolated pebbles that pass upwards into red silts and sands, as proved in borehole ITGE-3. Correlations between the boreholes and the seismic profiles allow the determination of the seismic character of the units (Figs. 4 and 5). The units contain oblique and sigmoidal reflectors that downlap onto the underlying units, though channelled geometries are also observed, mainly towards the unit tops. The upper progradational units show oblique reflector configurations, which are interpreted to be caused by fluvial bars. Borehole ITGE-6 (Fig. 4) contains a sequence of five progradational units which, from the base, comprise: bioclastic coarse sand containing marine molluscs (unit d_0); coarse and medium sands (units d_1 and d_2); and red sands with scattered pebbles and silty sands (units d_3 and d_4). The lower units (units d_0, d_1 and d_2) are interpreted as consisting of delta-front and nearshore deposits, whilst the upper ones (units d_3 and d_4) are mostly interpreted as delta-plain deposits. The facies of the units change laterally both landwards and seawards. Seawards, the delta-front deposits of the lower units (in the basal part of units d_1, d_2 and d_3, as seen in borehole ITGE-1) consist of coarsening-upwards deposits: grey clayey silts and silts passing upward into grey fine sands, that are interpreted to be caused by progradation of a proximal prodeltaic facies. Seawards, these silts and sands thin into grey silts (as seen in borehole ITGE-2), interpreted to be of distal prodeltaic facies. In these two boreholes, the uppermost units (d_4 and d_5) comprise coarse sands that are interpreted to be of delta front facies which overlap the finer facies of the underlying units. The boreholes are located at the apices of the two main delta lobes identified in historical mapping (Maldonado, 1972); ITGE-1 over the Riet-Vell lobe, which was active between 1100 and 1300 A.D., and ITGE-2 over the Mitjorn lobe which formed as a result of lobe switching at about 1700 A.D. The delta-front facies of unit d_4 was generated by these two progradational lobes. A conspicuous erosional surface, marked by channelling, is identified on seismic profiles between units d_3 and d_4. On the seismic profile (Fig. 2), the delta-front facies, with oblique reflectors, of unit d_3 appear to have been eroded by the Mitjorn channel of unit d_4. Landwards, the delta-front deposits pass into red sands with scat-

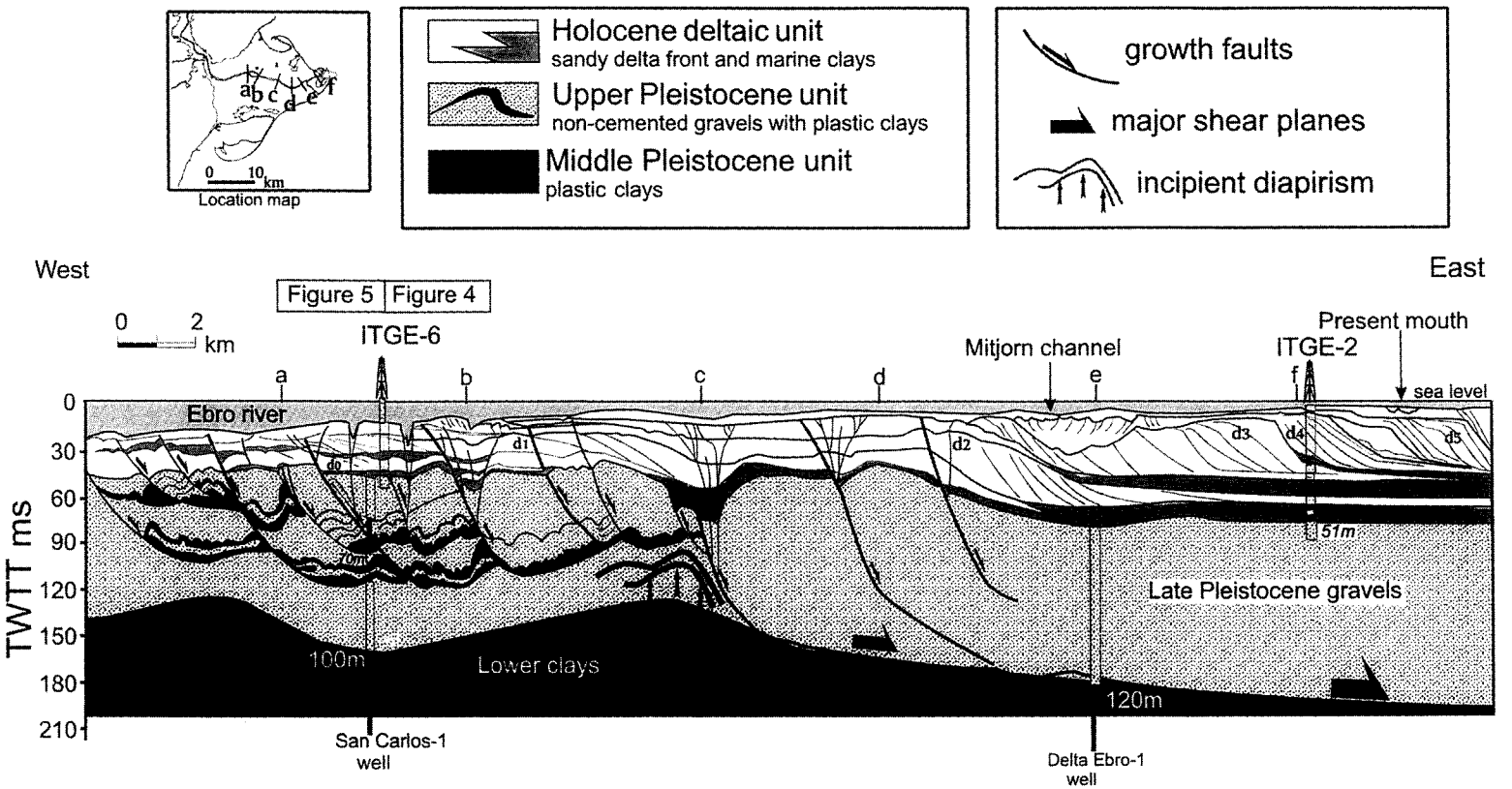

Fig. 2. Deformation structures and sedimentary geometry of the Late Pleistocene–Holocene deposits beneath the Ebro delta based on the interpretation of the high-resolution seismic profile along the Ebro and well-log correlation. Vertical scale is in milliseconds (ms) two-way travel time (TWTT). The locations of Figs. 4 and 5 are also shown.

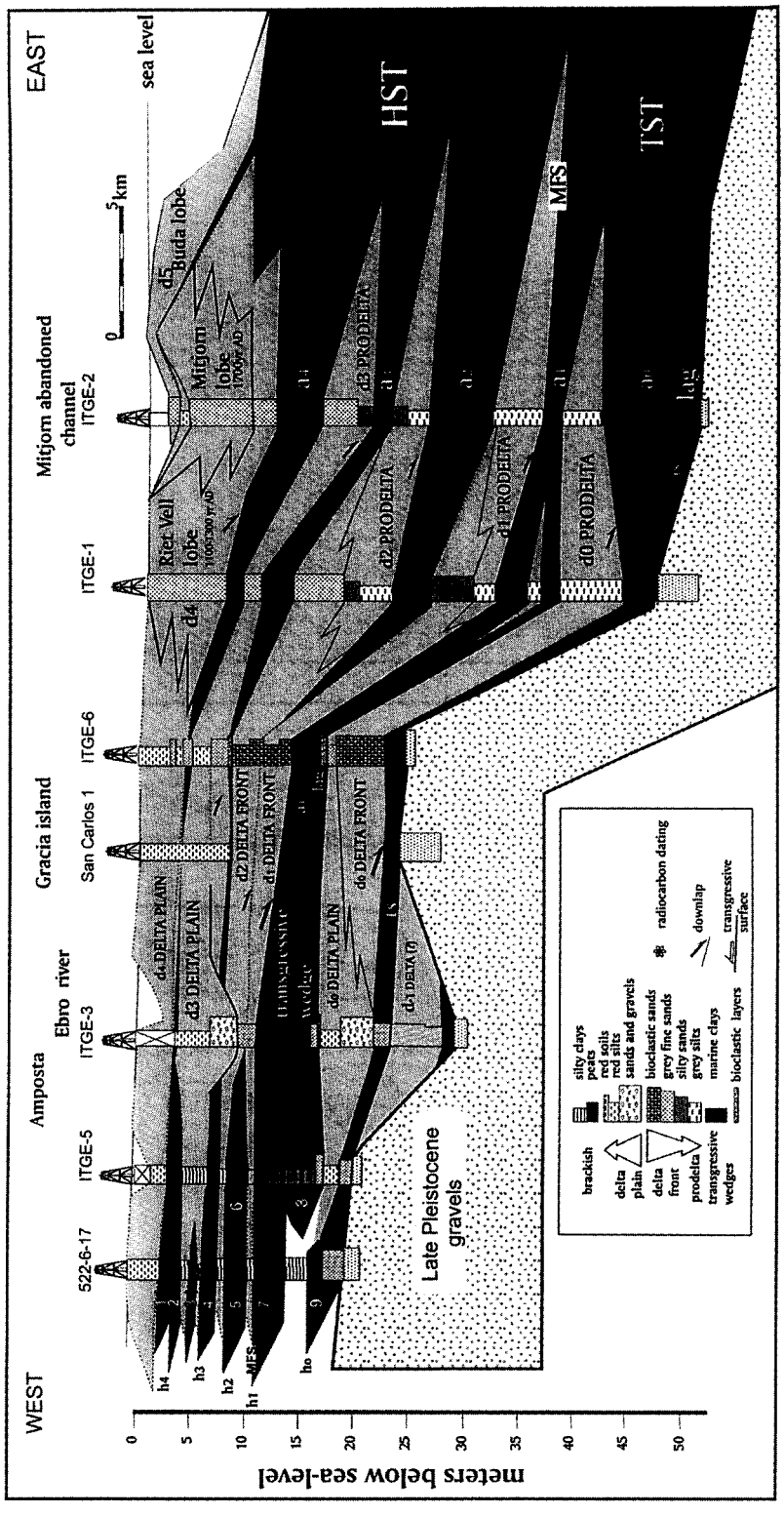

Fig. 3. Well-log correlation of Holocene sedimentary units beneath the Ebro delta plain. Deposits with a darker ornament are aggradational (marine clay wedges, inland peats), whereas those with a paler ornament are progradational deltaic deposits.

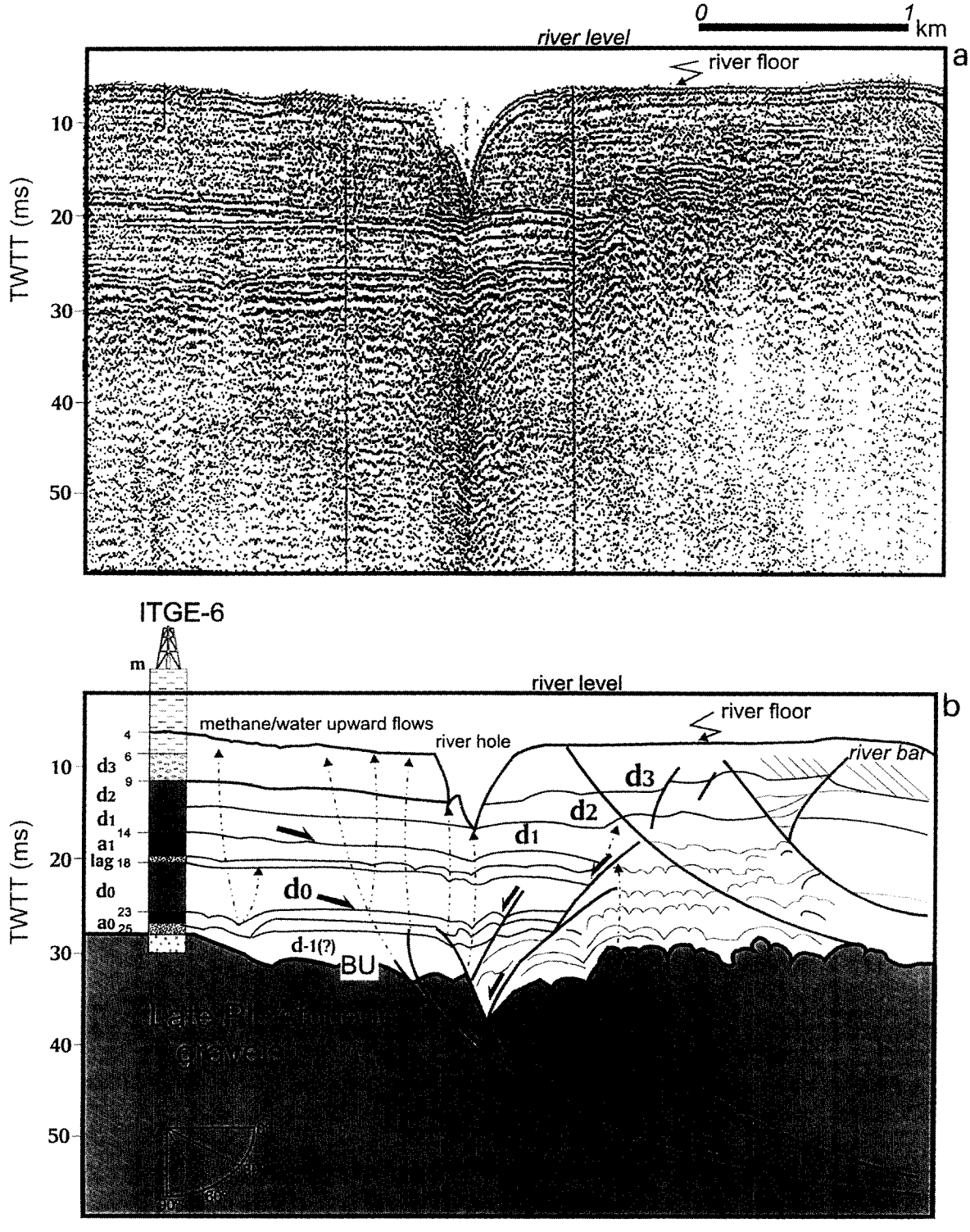

Fig. 4. Interpretation of a section of the high-resolution seismic profile along the Ebro in conjunction with the log of borehole ITGE 6. The vertical scale is in milliseconds (ms) two-way travel time (TWTT). See Fig. 2 for location.

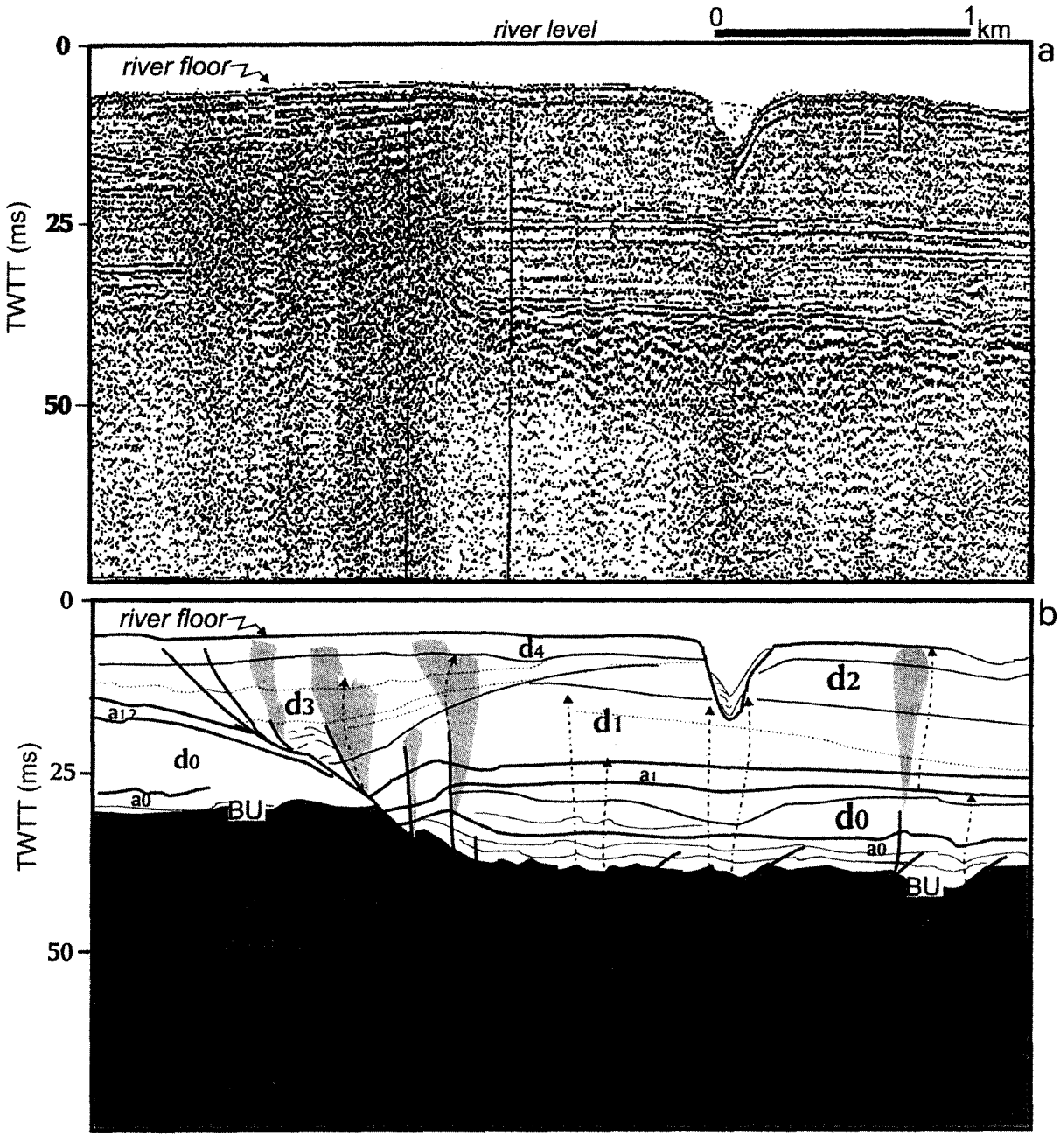

Fig. 5. Interpretation of a section of the high-resolution seismic profile along the Ebro. The vertical scale is in milliseconds (ms) two-way travel time (TWTT) See Fig. 2 for location.

tered pebbles and silts (cored in borehole ITGE-3) that are interpreted to be delta-plain and river-channel deposits. Towards the landward margin of the delta (boreholes ITGE-5 and 522-6-17), the delta-plain deposits pass into silty clays and organic silty clays, capped by gastropod-rich layers. These are interpreted to be flood-plain and freshwater-pond deposits, associated with the main river channel before

it reached the delta plain. The deposits contain thick peats that were deposited in freshwater to brackish environments.

The progradational units are interpreted to have been deposited as a succession of prograding delta lobes, with delta front and nearshore facies, which pass seawards into prodeltaic silts and sandy silts. Landwards they are formed of flood-plain, river-bar and channel deposits, represented by silts and organic silty clays with brackish to freshwater faunas. The bases of the progradational units are marked by downlapping. An erosional unconformity occurs at the top of each (particularly notable at the top of d_2) and is associated with the development of red soils and root traces. Seawards, the progradational prodeltaic deposits contain beds of shell debris towards their tops, which are interpreted to be transgressive lags that were overlapped by aggradational grey marine clays.

4.2. Aggradational deposits

4.2.1. Deltaic wedge-form facies

The aggradational 'a' units are composed of marine grey or black clays that overlie a basal mollusc shell lag. The units, best represented in boreholes on the seaward side of the delta (ITGE-1 and -2), have a landward-thinning wedge geometry. Units a_0 and a_1, which are interbedded with progradational sandy deposits (Figs. 4 and 5), are seismically transparent, or locally show parallel reflectors, bounded by high-amplitude reflectors. The aggradational units have high-amplitude reflectors at their bases which represent transgressive lag surfaces. The one at the base of unit a_1 corresponds, in borehole ITGE-6, with a 30–40-cm layer of shell debris. Unit a_0 onlaps the Late Pleistocene gravels (e.g. in borehole ITGE-6), and contains dome-like deformation structures, probably caused by methane or water escape (Figs. 4 and 5).

4.2.2. Inland peats

Landwards, aggradational deposits are represented by thick freshwater peats. A sequence of seven of these, interbedded with organic silts, were cored in boreholes ITGE-5 and 522-6-17 (Table 1) at depths between 16.5 and 2.0 m below mean sea-level (MSL). They have been radiocarbon-dated at between 8300 ± 300 and 1200 ± 50 yrs B.P. (Arasa, 1994). Aggradational unit a_1, which onlaps underlying units, is correlated with an inland peat at between 16.5 and 15 m below MSL, that has been radiocarbon-dated at between 8300 ± 300 (Arasa, 1994) and 7860 ± 350 (Solé et al., 1961) yrs B.P. The peat above this, dated at 6900 ± 100 yrs B.P., was penetrated 12 m below MSL and is correlated on log-wells with the top of unit a_1 (Fig. 3). The succeeding peat, drilled at 9 m

Table 1
Age, depth and sequence interpretation of samples which have been radiocarbon-dated from the Ebro delta

Index Nr.	^{14}C age (years B.P.)	Depth below MSL (m)	Dated material	Deltaic area	Sequence interpretation	Reference
1	1200 ± 50	2.5	Peat	Inland marsh	h_4c	Arasa, 1994
2	1800 ± 50	4.0	Peat	Inland marsh	h_4b	Arasa, 1994
3	2300 ± 100	5.2	Peat	Inland marsh	h_4a	Arasa, 1994
4	3300 ± 100	6.5	Peat	Inland marsh	h_3	Arasa, 1994
5	5180 ± 50	9	Peat	Inland marsh	h_2	Solé et al., 1961
6	5300 ± 100	9	Peat	Inland marsh	h_2	Arasa, 1994
7	6900 ± 100	12	Peat	Inland marsh	h_1	Arasa, 1994
	7950 ± 130		Shell	Prodelta	transgressive lag	Díaz et al., 1990
8	7860 ± 350	15	Peat	Inland marsh	h_0?	Solé et al., 1961
9	8300 ± 300	16.5	Peat	Inland marsh	h_0?	Arasa, 1994
	8800 ± 200		Shell	Prodelta	transgressive lag	Díaz et al., 1990
	9000 ± 200		Shell	Prodelta	transgressive lag	Díaz et al., 1990
	9300 ± 200		Shell	Prodelta	transgressive lag	Díaz et al., 1990
	9390 ± 190		Shell	Prodelta	transgressive lag	Díaz et al., 1990
	9570 ± 130		Shell	Prodelta	transgressive lag	Díaz et al., 1990
10	10320 ± 170	38	Peat	Prodelta	d-1?	Díaz et al., 1990

below MSL, was dated at between 5300 ± 100 (Arasa, 1994) and 5180 ± 50 (Solé et al., 1961) yrs B.P. and is correlated with unit a_2. The peat at 6.5 m below MSL, dated at 3300 ± 100 yrs B.P., has been correlated with unit a_3. The three uppermost peats, interbedded with silts and sand lenses, and drilled at 5.2 m, 4 m and 2.5 m depth below MSL have radiocarbon ages of 2300 ± 50, 1800 ± 50 and 1200 ± 50 yrs B.P., respectively. They are correlated with unit a_4, which is overlain landwards by fluvial deposits, and seawards by delta-front facies of progradational unit d_4.

The aggradational marine clays are interpreted to have formed as a consequence of a rapid increase in accommodation space in areas of moderate sediment supply during periods of rising sea-level. Such sea-level rises heightened the water table beneath the delta plain, causing pooling of nutrient-rich groundwaters that favoured the accumulation of peats and other organic sediments (frequent sea-level changes have been used as a mechanism to explain the variability of some littoral high-quality coals, interbedded with carbonaceous shales, in this manner; Kosters and Suter, 1993). The high rate of sea-level rise did not significantly favour the progradation of deltaic lobes. Instead, the sediments formed depositional wedges that onlap the prodeltaic facies of underlying deltaic lobes.

5. High-resolution sequence stratigraphy and high-frequency sea-level changes

The Holocene deposits of the delta may classically be interpreted as a Type 1 depositional sequence, being composed of (1) a transgressive systems tract (TST) overlying an unconformable sequence boundary, and (2) a highstand systems tract (HST). The lowstand systems tract is only represented on the outer shelf and slope by the Casablanca unit (Farrán and Maldonado, 1990) which is characterized by steep clinoforms that prograde onto the shelf. This unit contains sub-units, created by high-frequency relative sea-level changes, as have been reported along the southern Mediterranean Spanish coast (Hernandez-Molina et al., 1994). Its top is dated at 16,000 yrs B.P. (Nelson, 1990).

A relative mean sea-level curve (RMSL) has been constructed for the Ebro delta, based on sequence stratigraphic interpretations and radiocarbon-dated peats (see above, Table 1 and Fig. 6). For comparative purposes, a Holocene radiocarbon database, compiled from published data on the Mediterranean Spanish coast (Somoza et al., 1991; Zazo et al., 1994; Lario et al., 1995), has been used to construct a reference, non-deltaic, RMSL curve for the adjacent coastline (Fig. 6). Sea-level data mainly come from samples collected from beach and spit-bar systems, that formed during sea-level highstands along open coastlines, and correlate well with the Ebro inland peat index points. Five principal highstand sea-level events are recognised during the last 8000 years: h_1 (6900 to 6200 yrs B.P.); h_2 (5500 to 4400 yrs B.P.); h_3 (3900 to 2800 yrs B.P.); h_4 (2500 to 1100 yrs B.P.) and h_5 (600 yrs B.P. to present).

The RMSL curve for the Ebro delta can be correlated with that of the reference, non-deltaic curve, but it is greatly distorted by the local effects of subsidence. A subsidence rate of 1.75 mm per year produces the progressive sinking of the distinct asymmetric 'steps' in the curve that are related to high-frequency eustatic cycles (Fig. 6). The depositional units are interpreted in terms of these steps; the aggradational (a) units are represented by the transgressive segment of each 'step'. The subsequent deceleration in sea-level favours peat formation immediately before the peak of the relative highstand (h units). The following eustatic regressive phase generates a stillstand, or a smooth fall in relative sea-level, which is enough to increase river gradients and reduce accommodation space. These conditions favour the development and progradation of delta lobes (d units). The progradational deposits of the delta may thus have formed in stillstand segments of the relative sea-level curve within periods of falling global (eustatic) sea-level.

Sequence stratigraphic analysis shows that the RMSL of the delta may be interpreted as being controlled by high-frequency eustatic fluctuations that have been modified by local subsidence processes. These eustatic fluctuations, in the order of 1000 year magnitude, constitute 5th-order sequences, which modify both the 4th-order TST and HST.

5.1. Progradational episodes within the TST

The TST deposits of the delta comprise the aggradational a_0 and a_1 units and the progradational

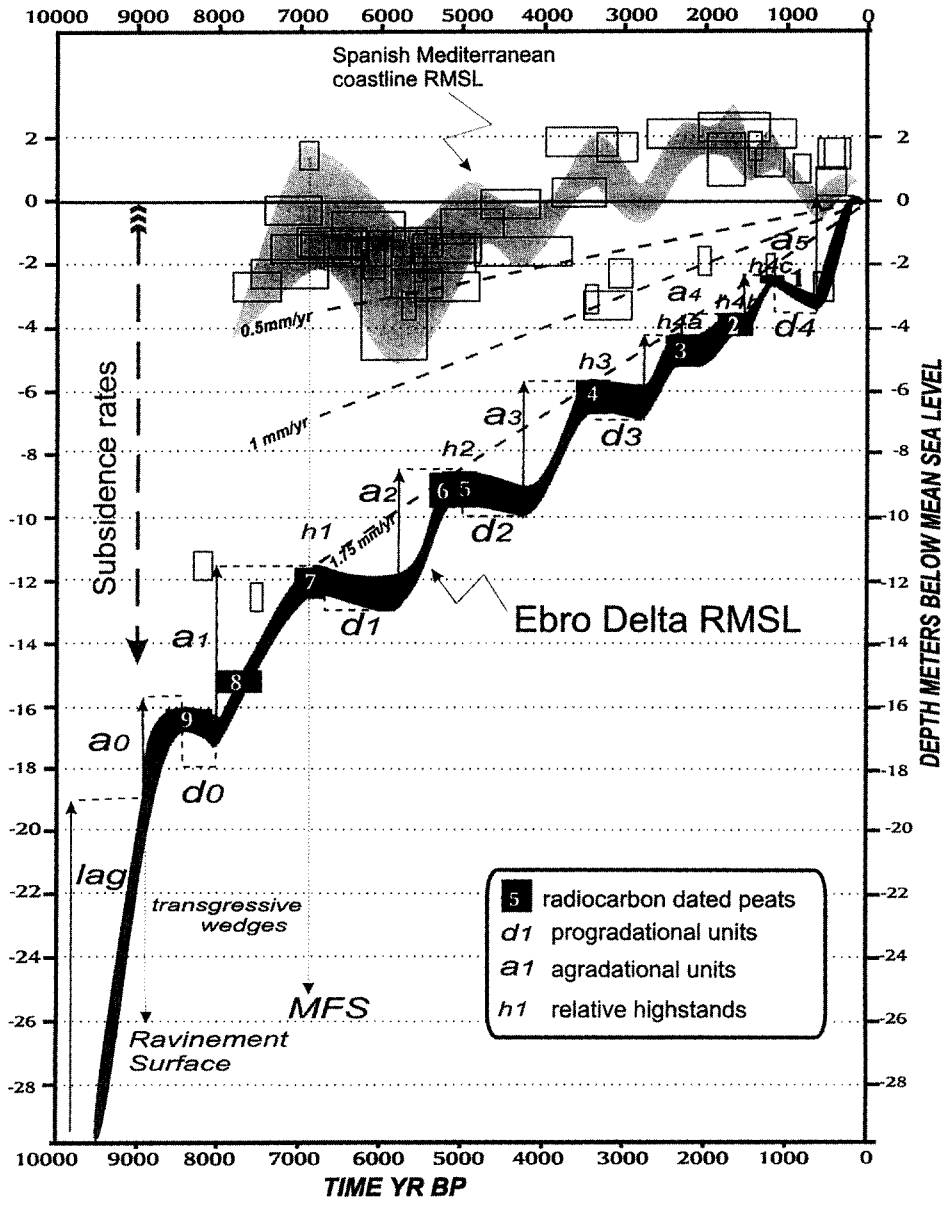

Fig. 6. Relative mean sea-level (RMSL) curve and stratigraphical signatures of Holocene sequences of the Ebro delta and adjacent coast. Index points of radiocarbon-dated peats are listed in Table 1. The linear subsidence rate of 1.75 mm per year fits the main RMSL trend over the last 7000 years. The upper curve corresponds to the RMSL for nearshore deposits on the adjacent Mediterranean Spanish coast. High-frequency sea-level oscillations (fifth to sixth order) may be correlated between the two RMSL curves.

d_0 unit. These are interpreted as retrogradational transgressive parasequences, each of which contains a lower aggradational transparent wedge, with basal transgressive lag, and an upper progradational unit. The TST deposits also include retrogradational parasequences, observed on the middle shelf, which correspond to the Late Pleistocene and Holocene Coves unit of Farrán and Maldonado (1990). The landward stacking of retrogradational deltaic bodies in a transgressive system overlapping the shelf is

hierarchically and cyclically controlled by periods of stillstand or minor falls during the Late Pleistocene–Holocene sea-level rise (Hernandez-Molina et al., 1994). Major stillstands have been reported on the Ebro shelf and in the Gulf of Lyon at about 10,500 yrs B.P. and 15,000 yrs B.P. (Verdaguer, 1983; Alöisi, 1986; Díaz and Maldonado, 1990). A peat underlying the inner shelf prodelta mud at 38 m below MSL yielded an age of 10,320 ± 170 yrs B.P. (Díaz et al., 1990). It may represent the stillstand period at about 10,500 yrs B.P., which is associated with the Younger Dryas climatic event.

The mollusc-shell lag at the base of aggradational unit a_0 is interpreted to mark a transgressive surface that onlaps the Pleistocene basal gravels beneath the delta in a landward direction. Seawards, transgressive shelly sands, with numerous shell relicts, have been reported (Table 1) to have radiocarbon ages of 9300 ± 200, 9390 ± 190, 8800 ± 200 and 7950 ± 130 yrs B.P. (IGME, 1986; Díaz et al., 1990). A 5th-order eustatic fluctuation, which caused a deceleration in sea-level rise during the 4th-order transgressive segment, could be responsible for a peat dated at 8300 ± 300 yrs B.P., at 16 m below MSL. The subsequent regressive period associated with unit d_0 (see above and Fig. 3) is caused by a eustatic sea-level fall, such as have been reported in reefs at between 11 m (8500 yrs B.P.) and 17 m (8200 yrs B.P.) below MSL during the main episode of Holocene sea-level rise (Larcombe et al., 1995).

The aggradational a_1 unit was deposited during the most extensive landward excursion of the sea during the Holocene. It overlies an unconformity at between 16 and 18 m below MSL, associated with mollusc-shell debris, that is interpreted to represent a transgressive surface onlapping the deposits of the preceding progradational episode (d_0). Landwards, the top of unit a_1 represents the maximum flooding surface (MFS), which marks the main inflection point of the 4th-order sea-level curve and divides the TST and HST. Radiocarbon dates of peats at the top of the unit (at 12 m below MSL) range between 7860 ± 350 (Solé et al., 1961; Macau, 1961) and 6900 ± 100 (Arasa, 1994) yrs B.P. Spit-bar systems along the Spanish Mediterranean coast started to prograde from the time of the MFS (6900 yrs B.P., Lario et al., 1995) onwards.

5.2. Progradational/aggradational episodes within the HST

The HST which overlies the MFS (Fig. 3), is composed of five progradational units (d_1, d_2, d_3, d_4 and d_5) and four aggradational units (a_2, a_3, a_4 and a_5) that are arranged into progradational parasequences. The progradational units, showing downlapping onto their bases and erosional unconformities at their tops, are interpreted to represent episodes of sea-level stillstand, or slight falls, during a period of overall sea-level highstand. The aggradational units have landward-thinning wedge geometries. Their bases are marked by mollusc-shell horizons that are interpreted to represent minor transgressive surfaces. Landwards, thick peats, named h_1 to h_4, are interpreted to have started forming under conditions of rising groundwater, caused by sea-level rise, immediately before the maximum flooding event. Marine clays (a) and thick peats (h) are thus both the aggradational response to sea-level rise because of an increase in accommodation space.

6. Subsidence rates and relative sea-level

The RMSL curve for the delta shows that the delta has had a notable rate of subsidence (illustrated by the progressive sinking of the maximum peaks) relative to the adjacent nearshore deposits (Fig. 6). The curve for the delta may be fitted to a linear subsidence rate of 1.75 mm per year relative to present sea-level. Similar subsidence rates reported for other Holocene delta sequences include 1.5 mm per year, for the Nile delta (Stanley and Warne, 1993) and between 1.6 and 4.0 mm per year for the Yangtze delta (Stanley and Chen, 1993). By taking the subsidence rate into account, and eliminating the 5th-order oscillations, a 'theoretical' 4th-order eustatic curve can be reconstructed by 'decompacting' the RMSL curve (Fig. 7). The theoretical curve allows us to analyse the 4th-order sequence stratigraphical trends of the delta. The part of the curve which represents the period between 10,000 and 8800 yrs B.P. is related to the development of the ravinement surface (Swift, 1968) with shell lags, above the basal gravels. The subsequent deposition of the a_0 and a_1 transgressive aggradational wedges between 8800 and 6900 yrs B.P. was governed by increasing accommodation space and a

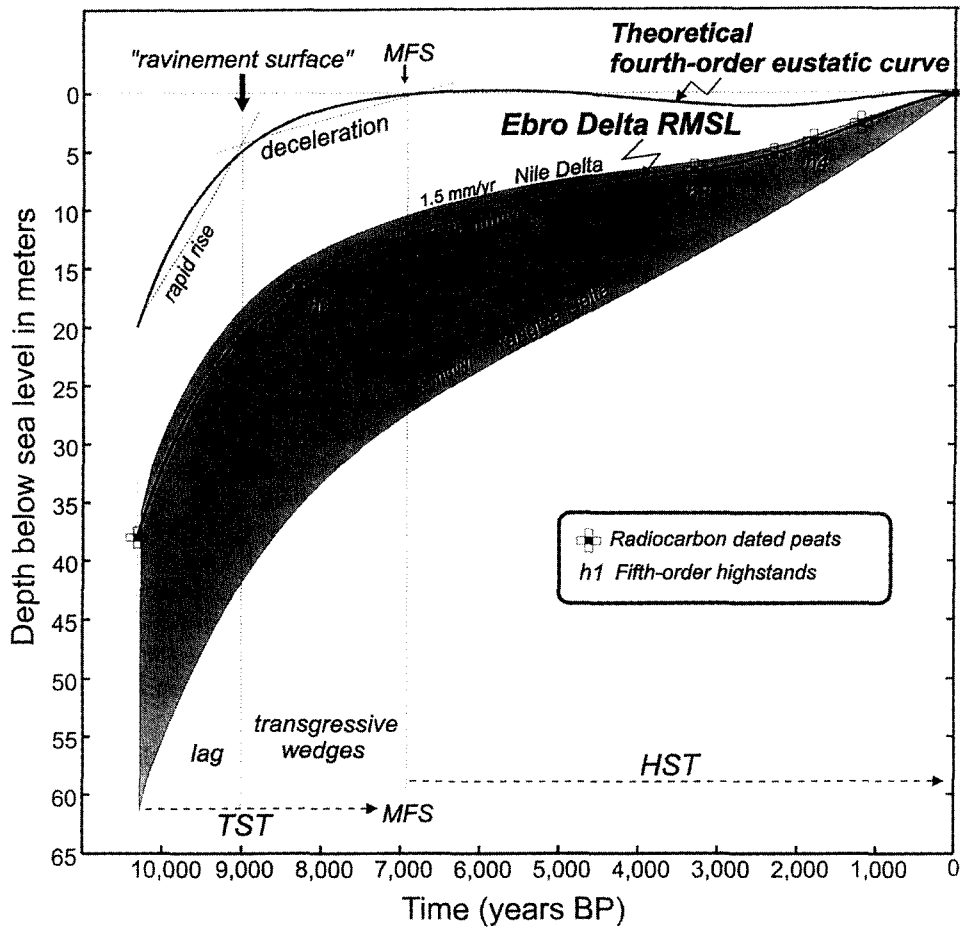

Fig. 7. Comparative subsidence rates of Holocene deltas. A theoretical fourth-order eustatic curve has been constructed by 'decompacting' the effects of subsidence (at an estimated rate of 1.75 mm per year) of the Ebro delta deposits. The main stratigraphical signatures observed are related to the fourth-order eustatic trend. The rapid eustatic rise is associated with the transgressive lag and ravinement surface; deceleration is associated with the transgressive wedges and more rapid deceleration with the inflection point (the maximum flooding surface MFS) before the highstand system tract (HST).

steady rate of sediment supply. The sole progradational episode, represented by the d_0 deposits, within this interval of overall aggradation, is interpreted to be caused by a 5th-order sea-level oscillation. The inflection point of the 4th-order eustatic curve, at between 6900 and 6700 yrs B.P., coincides with the first time that sea-level rose above present MSL during the Holocene. This event, dated by the first appearance of mangrove roots at 6610 yrs B.P. (^{14}C), 7500 yrs B.P. (sidereal) or at 5500 BC (calendar years) (Geyh et al., 1979), marks the MFS and the boundary between the 4th-order TST and HST. The HST is dominated by progradational delta lobes that were caused by 5th-order fluctuations; the aggradational deposits between these result from the high subsidence rate of the delta, which created the accommodation space needed for sediment aggradation.

The theoretical 4th-order eustatic curve (Fig. 7) suggests that the worldwide initiation of deltas was not caused by an asymptotic deceleration in sea-level up to the present, as proposed by Stanley and Warne (1994), but instead by rapid deceleration and subsequent stabilisation of the 4th-order sea-level trend. The asymptotic curve used to explain the worldwide initiation of deltas by eustasy (Warne and Stanley, 1995), must be interpreted in terms of a 4th-order

relative sea-level curve which is modified locally by subsidence processes with ranges of up to 4.0 mm per year in deltaic environments (Fig. 7). High subsidence rates produce the relative stacking, and preservation, of the 5th-order parasequences (mainly dominated by aggradational deposits during the TST and by progradational lobes during the HST) of the 4th-order sequence. The stacking allows us to explain the wide range of ages for the initiation of deltas based on 'basal peats' (between 8500 and 6500 yrs B.P.). In our opinion, these basal peats were generated by 5th-order fluctuations within the 4th-order TST, whereas the main progradation of deltas began at the 4th-order inflection point at around 6900 yrs B.P.

7. Discussion: the creation of progradational deltaic lobe pulses by global high-frequency fluctuations

The role of 5th- and 6th-order eustatic fluctuations in influencing the development and evolution of deltas worldwide has been widely discussed (Stanley and Warne, 1994; Lowrie and Hamiter, 1995). However, the global correlation between accurately radiocarbon-dated deltaic episodes to clarify the role of high-frequency eustatic oscillations on delta architecture, has been neglected. Lowrie and Fairbridge (1991), in their work on the Mississippi delta, were the first to note the role of eustatic and climatic–hydraulic controls on delta architecture. They noted the relationship between high ^{14}C fluxes, cold events (reflecting lower solar intensity) and a lowered MSL, and low ^{14}C fluxes, warm events and a high MSL. An examination of the record of solar activity (documented by ^{14}C fluxes levels in tree rings: Stuiver and Braziunas, 1989) suggests the existence of at least 38 cycles over the last 10,700 years (about one every 275 years), representing a 6th-order frequency (Lowrie and Hamiter, 1995). The record identifies 16 cycles (in clusters) of 5th-order frequency that were so extreme that they caused 'neoglacial' events (e.g. the global climatic cooling event at 3321 B.C., associated with the Sumerian ^{14}C peak, and that at 1682 A.D., named the Maünder Minimum, related to the Little Ice Age climatic deterioration), which caused a drop in sea-level.

Such 5th- or 6th-order cycles should regionally not only affect sea-level, but also sediment supply parameters. Therefore, in the case of the Ebro delta, short cool/humid events should produce both: (1) a sea-level fall (because of expanding ice cover), a decrease in Mediterranean sea-surface water temperatures, and a decrease in the flux of waters from the Atlantic into the Mediterranean Sea; and (2) an increase in sediment supply by increasing precipitation within the Ebro drainage basin (including the Pyrenees). The rapid (albeit limited) drop in MSL during such events, would cause incision of the main river channel and 'ravinement' of the unconsolidated delta plain, thus favouring progradation of the delta-front lobes when sediment supply exceeds accommodation (Thorne and Swift, 1991). By way of contrast, warming events, forcing a rise in sea-level, should decrease sediment supply to the Ebro delta by increasing prevailing anticyclonic conditions over the Iberian Peninsula. The decrease in sediment supply, allied with a decrease in hydraulic gradient, favours channel switching on the delta plain, and the rapid abandonment of the main delta lobes. Such an event, marked by a sea-level rise of 0.5–0.6 m above MSL, occurred during the Viking period, about 1000 years ago. The landward migration of saltwater wedges increased the accumulation of inter-distributary sediment by frequent flooding of the delta-plain and by hampering the flux of fresh groundwaters under the delta-plain, generated freshwater peats inland.

A tentative chronology of the high-frequency climatic–eustatic oscillations influencing deltaic sedimentation over the last 7000 years is proposed (Fig. 8). It is based on: (1) highstand peaks (h episodes) from the Mediterranean and southern Atlantic coasts of Spain (Somoza et al., 1991; Zazo et al., 1994); (2) the stratigraphical sequence of radiocarbon-dated peats (index points 1 to 10; Table 1) and progradational lobes in the Ebro delta; and (3) the regressive episodes of the Mississippi delta (Frazier, 1967; Fairbridge, 1988; Lowrie and Fairbridge, 1991). Highstand episodes, related to beach and spit-bar growth, are defined by the highest values of the radiocarbon data frequency histogram, whilst gaps are associated with lowstand stages. Radiocarbon-dated peats 7 and 8 formed during aggradational episodes, within a period of rising sea-level, just before the Holocene maximum flooding event (Fig. 8). Inland, peats 1 to 6 are interpreted to be related to relative maximum flooding stages, and coincide

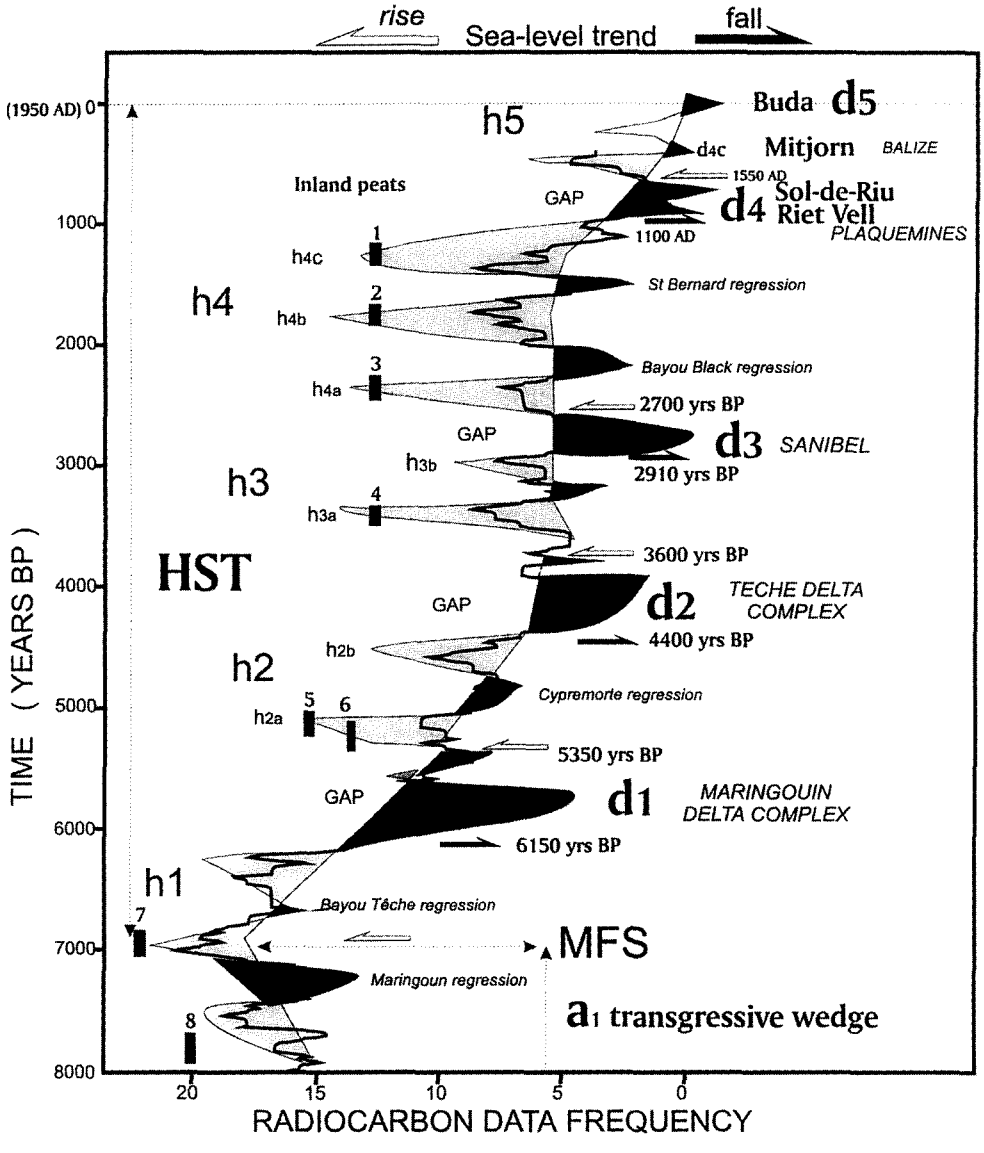

Fig. 8. Tentative chronology of high-frequency climatic–eustatic swings over the last 8000 years, based on the correlation between: (a) radiocarbon-dated peats and the historical chronology of lobe progradation of the Ebro delta; (b) the histogram of radiocarbon data from nearshore deposits of the Spanish Mediterranean coast (partly modified from Somoza et al., 1991; Zazo et al., 1994); and (c) the chronology of the main delta complexes and regressive episodes of the Mississippi delta (Fairbridge, 1988; Lowrie and Fairbridge, 1991). The *h* episodes are interpreted as warm events, with a high MSL. These are followed by cold periods, of lowered MSL, which controlled progradation of the main delta complexes (*d* episodes). These delta complexes were caused by fifth-order fluctuations (of thousand-year magnitude); sixth-order fluctuations (of hundred-year magnitude) caused switching of delta lobes within them.

with highstand peaks (h_1, h_2a, h_3a and h_4). The gaps between the highstand peaks correspond with the main progradational lobes of the Ebro delta (d_1, d_2, d_3, d_4 and d_5) (Fig. 8), and are interpreted to have formed by sea-level stillstand, or slight falls, after the maximum flooding stage. This chronology matches well the episodes of deltaic progradation in the Mississippi delta. Thus, the d_1 unit correlates with the

Maringouin complex (6150–5350 yrs B.P.) between the h_1 and h_2 relative highstands. The d_2 unit corresponds with the Têche delta complex (4400–3600 yrs B.P.) between the h_2 and h_3 maxima. The d_3 unit fits with the Sanibel regression (2910–2700 yrs B.P.), also called Sanibel I (Stapor et al., 1991), between the h_3 and h_4 maxima. The d_4 progradational unit consisting of the Riet Vell (1100–1300 A.D.) and Sol-de-Riu lobes (1350–1700 A.D.) coincides with the Plaquemines regression (1100–1350 A.D.), also called Sanibel II (Stapor et al., 1991). The Mitjorn lobe, active around 1700 A.D., coincides with the Balize regressive pulse (1750 A.D.). The development of the modern Balize sub-delta has been related to a small-amplitude sea-level fall of between 0.5 and 1 m below present MSL; this is associated with the neoglacial event of the 'Little Ice Age' between about 1600 and 1800 A.D. (Swift et al., 1991). Kosters and Suter (1993) consider that the Maringoun/Têche delta complexes of the Mississippi delta belong to the TST, because they are overlain by a transgressive lagoonal facies after 3500 yrs B.P. However, these complexes, and their correlatives in the Ebro delta, should be considered as major progradational events within the 4th-order HST. The flooding surface that onlaps these complexes should be regarded as a minor MFS before the h_3 highstand. This surface, separating the h_1 and h_2 systems from the h_3, h_4 and h_5 systems of the HST during the last deglaciation, has been reported elsewhere on the Spanish shelf (Hernandez-Molina et al., 1994). The correlation between the Ebro and Mississippi delta progradation stages supports the existence of periodic sea-level fluctuations that were forced by rapid global climate changes.

The geometry of the Ebro delta was created by the advance of successive subdelta lobes which prograded radially seawards from an avulsion point across the lowest lateral zones of the delta-plain during regressive stages (Fig. 9). An abrupt fall in sea-level, following a period of eustatic rise, has an important role in delta-lobe switching by creating appropriate conditions for rivers to leave their established channels during a major flood (Lowrie and Hamiter, 1995). In the case of the Ebro delta, the main delta-lobe progradational events have frequencies of thousand-year magnitude that are related to 5th-order oscillations (Fig. 8). Modification of the different delta lobes may be related to 6th-order eustatic oscillations (of hundred-year magnitude). This chronology tallies with that of other deltas, such as that of the Rhine and Meuse (which also has a comprehensively radiocarbon-dated C^{14} histogram) that indicates that most intra-avulsion periods were in the order of 1000 years, although values of 500 and 5000 years also occurred (Tornquist, 1994).

Episodes of sea-level rise are related to periods of sediment aggradation. During such episodes, the flooding and reworking of distributary channels and delta lobes, transformed the delta complexes into shoreline sand bodies and inner-shelf shoals (Penland et al., 1988; Kosters and Suter, 1993). The sea-level rises which followed the progradation of the Sol-de-Riu and Mitjorn progradation lobes (the Plaquemines and Balize regression events of the Mississippi delta) caused the growth of the southern La Banya and Trabucador spit-bar (by destruction of the Riet Vell lobe) and the northern El Fangar spit-bar (by destruction of the Sol-de-Riu lobe) in the 17th and 18th centuries. Warm periods in the 18th century (related to sunspot maxima of $R_M = 158$ in 1778 A.D. and $R_M = 141$ in 1788 A.D.; R.W. Fairbridge, pers. commun., 1996) coincide with the main period of growth of the La Banya spit-bar, which took place between about 1740 and 1813 A.D. (Fig. 9).

8. Conclusions

(1) During the Late Pleistocene and Holocene a Type 1, 4th-order, depositional sequence was created worldwide. The Ebro delta consists of TST and HST deposits which formed during the Holocene part of the sequence.

(2) Rapid sea-level rise between 10,000 and 8800 yrs B.P., and rapid shoreline migration, formed a ravinement surface and associated shell lag on the top of Pleistocene basal gravels. This surface is onlapped by the TST deposits, which are characterized by retrogradational stacking of high-frequency sequences. A deceleration in the rise of sea-level between 8800 and 6900 yrs B.P. favoured the deposition of transgressive aggradational wedges (a_1 and a_0 units). Deltaic lobes separating these were caused by progradation associated with 5th-order oscillations.The top of the uppermost (a_1) unit is interpreted to be the Holocene 4th-order MFS. Peats

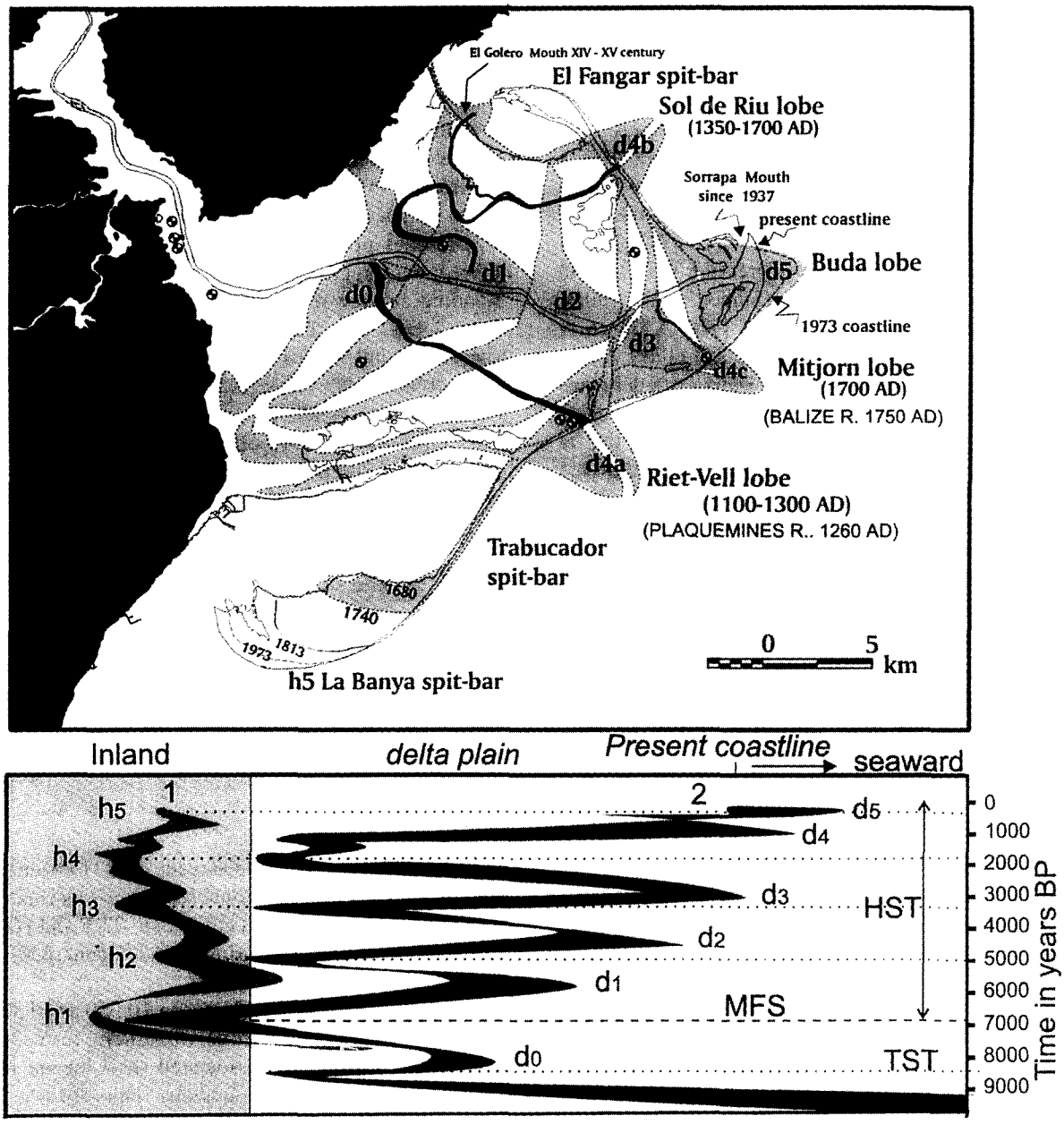

Fig. 9. Map showing a reconstruction of the Holocene evolution of the Ebro delta lobes based on correlation between well logs, high-resolution seismics, electric subsurface conductivity maps and historical data of the Ebro delta. The lower figure shows migration of the delta fronts through time by the progressive development of the delta complex during lowstand phases (*d* episodes).

in the inner delta which correlate with this unit have been radiocarbon-dated at between 7860 ± 350 and 6900 ± 100 yrs B.P.

(3) The HST deposits, which overlie the MFS, comprise five progradational delta units (d_1, d_2, d_3, d_4 and d_5) and four aggradational units (a_2, a_3, a_4 and a_5) which have an overall progradational stacking pattern. Major progradational events during the

HST have a chronology that matches the regressive episodes of the Mississippi delta, which are intercalated between relative highstands: (1) the d_1 delta progradation is correlated with the Maringouin complex (6150 to 5350 calender yrs B.P.) between the h_1 and h_2 relative highstands; (2) the d_2 delta progradation is correlated with the Teche delta complex (4400 to 3600 yrs B.P.) between the h_2 and h_3 maxima; (3) the d_3 delta progradation is correlated with the Sanibel regression (2910 and 2700 yrs B.P.), between the h_3 and h_4 maxima; and (4) the d_4 deltaic progradation, responsible for the Riet-Vell and Sol-de-Riu lobes, active between 1100 and 1300 and 1350 to 1700 A.D., is correlated with the Plaquemines regression (1100 to 1350 AD). The last regressive pulse, (the Balize regression), at about 1750 A.D., coincides with the development of the Mitjorn lobe around 1700 A.D.

(4) 5th- to 6th-order sea-level cycles modulate both the TST and HST, forming retrogradational and progradational high-frequency sequences respectively, and give rise to a 4th-order composite sequence. The main delta-lobe progradational events have frequencies of thousand-year magnitude which are related to 5th-order oscillations. Modifications of the delta lobes may be related to 6th-order eustatic oscillations of hundred-year magnitude.

(5) The RMSL curve constructed for the Ebro delta shows that high-frequency eustatic cycles were distorted progressively by subsidence. The linear trend fitted to the curve shows that subsidence rates of 1.75 mm per year have prevailed during the last 7000 years. Subsidence produces a 'stepped' curve where each step correlates with a highstand episode in adjacent nearshore deposits of the Spanish Mediterranean coastline. The stacking patterns observed in the delta result from high-frequency sea-level (and sediment-supply) changes in a setting where accommodation space is continuously increased by subsidence. Subsidence rates allow the stacking, and preservation, of successive progradational deltaic deposits, formed during the relative lowering of sea-level.

Acknowledgements

Special thanks to Rhodes W. Fairbridge and Allen Lowrie for their appreciated letters and helpful comments. The manuscript also benefited from the useful critical reviews by R. Hamiter, B. Gensous, T.B. Roep, C.D.R. Evans, and D.J. Evans. This research was carried out by the financial support of the CEDEX (Spanish Harbour and Coastal Modelling Laboratory) and ITGE (Geological Survey of Spain). Thanks are also due to the IEO (Oceanographic Spanish Institute) for supplying marine geophysical equipment. This paper is published with the permission of the Directors of the Geological Survey of Spain (ITGE) and British Geological Survey (NERC) and is a contribution to the International Geological Correlation Programme (IGCP) Project 396, Continental Shelves in the Quaternary.

References

Alöisi, J.C., 1986. Sur un modèle de sédimentation deltaique. Contribution à l'étude des marges passives. Thesis, University of Perpignan, 162 pp.

Arasa, A., 1994. Estratigrafia i sedimentologia dels materials Plio–Quaternaris del Baix-Ebre i sectors adjacents. Doctoral Thesis, University of Barcelona, 447 pp. (unpublished).

Belloti, P., Chiocci, F.L., Milli, S., Tortora, P., Valeri, P., 1994. Sequence stratigraphy and depositional setting of the Tiber Delta: integration of high-resolution seismics, well logs, and archeological data. J. Sediment. Res. B 64 (3), 416–432.

Boyd, R., Suter, J., Penland, S., 1989. Sequence stratigraphy of the Mississippi Delta. Trans. Gulf Coast Assoc. Geol. Soc. 39, 331–340.

Checa, A., Diaz, J.I., Farran, M., Maldonado, A., 1988. Sistemas Deltaicos Holocenos de los rios Llobregat, Besos y Foix: Modelos Evolutivos Transgresivos. Acta Geol. Hisp. 23, 241–255.

Coleman, J.M., Prior, D.B., Lindsay, J.F., 1983. Deltaic influences on shelf edge instability processes. In: Stanley, D.J., Moore, G.T. (Eds.), The Shelfbreak: Critical Interface on Continental Margins. Soc. Econ. Paleontol. Mineral. Spec. Publ. 33, 121–137.

Crans, W., Mandl, G., Haremboure, J., 1980. On the theory of growth faulting: a geomechanical delta model based on gravity sliding. J. Pet. Geol. 2, 265–307.

Dansgaard, W., White, J.W.C., Johnson, J., 1989. The abrupt termination of the Younger Dryas Climate Event. Nature 339, 532–534.

Díaz, J.I., Maldonado, A., 1990. Transgressive sand bodies on the Maresme continental shelf, Western Mediterranean. Mar. Geol. 91, 53–73.

Díaz, J.I., Nelson, C.H., Barber, J.H., Jr., Giro, S., 1990. Late Pleistocene and Holocene sedimentary facies on the Ebro continental shelf. In: Nelson, C.H., Maldonado, A. (Eds.), The Ebro Continental Margin, Northwestern Mediterranean. Mar. Geol. 95, 333–352.

Fairbridge, R.W., 1961. Eustatic changes in sea level. Phys. Geochem. Earth 4, 99–185.

Fairbridge, R.W., 1988. Mississippi delta-lobe switching during Holocene eustatic fluctuations. Am. Assoc. Pet. Geol. Bull. 72, 183–184.

Farrán, M., Maldonado, A., 1990. The Ebro continental shelf: Quaternary seismic stratigraphy and growth patterns. In: Nelson, C.H., Maldonado, A. (Eds.), The Ebro Margin Continental Margin, Northwestern Mediterranean. Mar. Geol. 95, 289–312.

Field, M.E., Gardner, J.V., 1990. Pliocene–Pleistocene growth of the Rio Ebro margin, northeast Spain: a prograding-slope model. Geol. Soc. Am. Bull. 102, 721–733.

Frazier, D.E., 1967. Recent deltaic deposits of the Mississippi River their development and chronology. Trans. Gulf Coast Assoc. Geol. Soc. 17, 287–315.

Galloway, W.E., 1975. Process framework for describing the morphologic and stratigraphic evolution of deltaic depositional systems. In: Broussard, M.L. (Ed.), Delta Models For Exploration. Houston Geological Society, Houston, Texas, pp. 87–98.

Gensous, B., Tesson, M., 1992. High-resolution sequence stratigraphy of the Late Quaternary Rhone shelf deposits: relations with tectonic and eustasy; reservoir implications. Int. Symp. Mesozoic and Cenozoic Sequence Stratigraphy of European Basins (abstr.), Dijon, pp. 446–447.

Gensous, B., Williamson, D., Tesson, M., 1993. Late-Quaternary transgressive and highstand deposits of a deltaic shelf (Rhône Delta, France). In: Posamentier, H.W., Summerhayes, C.P., Haq, B.V., Allen, G.P. (Eds.), Sequence Stratigraphy and Facies Associations. Spec. Publ. Int. Assoc. Sedimentol. 18, 197–211.

Geyh, M.A., Kudrass, H.R., Streif, H., 1979. Sea-level changes during the Late Pleistocene and Holocene in the Strait of Malacca. Nature 278, 441–443.

Guillén, J., Díaz, J.I., 1990. Elementos morfológicos en la zona litoral: ejemplos en el delta del Ebro. Sci. Mar. 54 (4), 359–373.

Hernandez-Molina, F.J., Somoza, L., Rey, J., Pomar, L., 1994. Late Pleistocene–Holocene sediments on the Spanish continental shelves: a model for very high-resolution sequence stratigraphy. Mar. Geol. 120, 129–174.

Hernandez-Molina, F.J., Somoza, L., Rey, J., 1996. Late Pleistocene–Holocene high-resolution sequence analysis on the Alboran Sea continental shelf. In: De Batist, M., Jacobs, P. (Eds.), Geology of Siliciclastic Shelf Seas. Geol. Soc. London, Spec. Publ. 117, 139–154.

Hydrotechnic Corporation, 1966. Proyecto de saneamiento y riegos del delta del Ebro: Reconocimiento de la viabilidad técnica y económica del drenaje del delta del Ebro y sustitución del cultivo de arroz por otros cultivos de regadío. Technical Report, Instituto Nacional de Colonización, Ministerio de Agricultura, Madrid, 450 pp. (unpubl.).

IGME, 1986. Mapa geológico de la plataforma continental española y zonas adyacentes. Escala 1:200000. Tortosa–Tarragona. Publication Instituto Geológico y Minero de España, Madrid, 78 pp., 3 maps.

IGME, 1987. Contribución de la exploración petrolífera al conocimiento de la geología de España. Publication Instituto Geológico y Minero de España, Madrid, 465 pp., 18 maps.

Jiménez, J.A., Sánchez-Arcilla, A., 1993. Medium-term coastal response at the Ebro delta, Spain. Mar. Geol. 114, 105–118.

Kindinger, J.L., 1988. Seismic stratigraphy of the Mississippi shelf and upper continental slope. Mar. Geol. 83, 73–94.

Kosters, C.A., Suter, R., 1993. Facies relationships and systems tracts in the Late Holocene Mississippi delta plain. J. Sediment. Petrol. 63, 727–733.

Lambeck, K., 1996. Shoreline reconstructions for the Persian Gulf since the last glacial maximum. Earth Planet. Sci. Lett. 142, 43–57.

Larcombe, P., Carter, R.M., Dye, J., Gagan, M.K., Johnson, D.P., 1995. New evidence for episodic post-glacial sea-level rise, Central Great Barrier Reef, Australia. Mar. Geol. 127, 1–44.

Lario, J., Zazo, C., Dabrio, C.J., Somoza, L., Goy, J.L., Bardaji, T., Silva, P.G., 1995. Record of recent Holocene sediment input in spit-bars and delta plains of south Spain. In: Finkl, C.W., Jr. (Ed.), Holocene Cycles: Climate, Sea Levels and Sedimentation. J. Coastal Res. 17, 241–245.

Lowrie, A., Fairbridge, R.W., 1991. Role of eustasy in Holocene Mississippi Delta-lobe switching. In: Penland, S., Roberts, H.H. (Eds.), Coastal Depositional Systems in the Gulf of Mexico: Quaternary Framework and Environmental Issues. Program with Extended and Illustrated Abstracts, 12th Annu. Res. Conf., Gulf Coast Section, Soc. Econ. Paleontol. Mineral., pp. 111–115.

Lowrie, A., Hamiter, R., 1995. Fifth and sixth order eustatic events during Holocene, fourth order highstand influencing Mississippi delta-lobe switching. In: Finkl, C.W., Jr. (Ed.), Holocene Cycles: Climate, Sea Levels and Sedimentation. J. Coastal Res. 17, 225–229.

Macau, F., 1961. Contribución al estudio del Cuaternario en el Delta del Ebro. Bol. R. Soc. Esp. Hist. Nat. 59, 69–76.

Maldonado, A., 1972. El Delta del Ebro. Estudio sedimentológico y estratigráfico. Boletín de Estratigrafía, Universidad de Barcelona, Vol. 1, 474 pp.

Maldonado, A., 1975. Sedimentation, stratigraphy and development of the Ebro delta, Spain. In: Broussard, M.L. (Ed.), Delta Models For Exploration. Houston Geological Society, Houston, Texas, pp. 311–338.

Maldonado, A., Riba, O., 1971. El delta reciente del río Ebro: descripción de ambientes y evolución. Acta Geol. Hisp. 6 (5), 131–138.

Mandl, G., Crans, W., 1981. Gravitational gliding in deltas. In: McClay, K.R., Price, N.J. (Eds.), Thrust and Nappe Tectonics. Geol. Soc. London, Spec. Publ. 9, 41–54.

Miall, A.D., 1984. Deltas. In: Walker, R.G. (Ed.), Facies models, 2nd ed. Geoscience Canada Reprint Series, Geological Association Canada, pp. 105–118.

Mitchum, R.M., Jr., Van Wagoner, J.C., 1991. High-frequency sequences and their stacking patterns: sequence stratigraphic evidence of high-frequency eustatic cycles. Sediment. Geol. 70, 131–160.

Nelson, C.H., 1990. Estimated post-Messinian sediment supply and sedimentation rates on the Ebro continental margin, Spain.

In: Nelson, C.H., Maldonado, A. (Eds.), The Ebro Continental Margin, Northwestern Mediterranean Sea. Mar. Geol. 95, 395–418.

Nelson, C.H., Maldonado, A. (Eds.), 1990. The Ebro Continental Margin, Northwestern Mediterranean Sea. Mar. Geol. 95 (3/4), 1–442.

Penland, S., Boyd, R., Suter, J.R., 1988. Transgressive depositional systems of the Mississippi delta plain: a model for barrier shoreline and shelf development. J. Sediment. Petrol. 58, 932–946.

Posamentier, H.W., James, D.P., 1993. An overview of sequence stratigraphic concepts: uses and abuses. Spec. Publ. Int. Assoc. Sedimentol. 18, 3–18.

Posamentier, H.W., Jervey, M.T., Vail, P.R., 1988. Eustatic controls on clastic deposition I-Conceptual Framework. In: Wilgus, C.K., Hastings, B.S., Kendall, C.G.St.C., Posamentier, H., Ross C.A., Van Wagoner, J. (Eds.), Sea-Level Changes — An Integrated Approach. Soc. Econ. Paleontol. Mineral. Spec. Publ. 42, 109–124.

Postma, G., 1995. Sea-level related architecture trends in coarse grained delta complexes. In: S.K. Chough and Orton, G.J. (Eds.), Fan Deltas: Depositional Styles and Controls. Sediment. Geol. 98, 3–12.

Rao, P.S., Rao, G.K., Rao, N.V., Swamy, A.S.R., 1990. Sedimentation and sea-level variations in Nizampatnam Bay, East Coast of India. J. Indian Sci. 19, 261–264.

Rodriguez-Ortiz, J.M, Castañedo, F.J., Prieto, C., Hermoso, J., 1978. The evolution of the Ebro Delta. 3rd Int. Congr. Assoc. Eng. Geol., Madrid, pp. 248–260.

Scruton, P.C., 1960. Delta building and the deltaic sequence. In: Shepard, F.P., Phleger, F.B., Van Andel, T.H. (Eds.), Recent Sediments, Northwestern Gulf of Mexico. Am. Assoc. Pet. Geol., Tulsa, Okla., pp. 82–102.

Serra, J., Riera, G., 1993. La desembocadura del río Ebro: variabilidad y cambios recientes. Geogaceta 14, 27–28.

Shepard, F.P, Phleger, F.B, Van Andel, F.H. (Eds.), 1960. Recent Sediments, Northwestern Gulf of Mexico. Am. Assoc. Pet. Geol., Tulsa, Okla., 394 pp.

Solé, L., Macau, F., Virgili, C., Llamas, M.R., 1961. Algunos datos sobre la evolución sedimentaria del Delta del Ebro. 2ª Reunión de Sedimentologia, Inst. Edafologia, CSIC, Madrid, pp. 197–199.

Soler, R., Martínez, W., Megías, A.G., Abeger, J.A., 1983. Rasgos básicos del Neógeno del Mediterráneo español. Mediterranea Ser. Geol. 1, 71–82.

Somoza, L., Rey, J., 1993. Holocene fan-deltas in a Ria morphology. In: Dabrio, C.J., Zazo, C., Goy, J.L. (Eds.), Fan Deltas: The Dynamics of Coarse Grained Deltas. Cuad. Geol. Iber. 15, 37–48.

Somoza, L., Goy, J.L., Zazo, C., Bardaji, T., Dabrio, C.J., Silva, P.G., Lario, J., 1991. Holocene sea-level highstands in the Western Mediterranean, SE Spain. A computer-statistical analysis of radiocarbon dating. Mediterranean and Black Sea shorelines Subcomm. INQUA Newsl. 13, 61–64.

Somoza, L., Hernandez-Molina, F.J., Andres, J.R., Rey, J., 1997. Continental shelf architecture and sea-level cycles: Late Quaternary high-resolution stratigraphy of the Gulf of Cadiz (Spain). Geo-Mar. Lett. 17, 133–139.

Stanley, D.J., Chen, Z.Y., 1993. Yangtze delta, Eastern China. Geometry and subsidence of a Holocene depocenter. Mar. Geol. 112, 1–11.

Stanley, D.J., Warne, A.G., 1993. Nile Delta, recent geological evolution and human impact. Science 260, 628–634.

Stanley, D.J., Warne, A.G., 1994. Worldwide initiation of Holocene marine deltas by deceleration of sea-level rise. Science 265, 228–231.

Stapor, F.W., Mathews, T.D., Lindfors-Kearns, F.E., 1991. Barrier-island progradation and Holocene sea level history in Southwest Florida. J. Coastal Res. 7, 815–838.

Stuiver, M., Braziunas, T.F., 1989. Atmospheric ^{14}C and century-scale solar oscillations. Nature 338, 405–408.

Swift, D.J.P., 1968. Coastal erosion and transgressive stratigraphy. J. Geol. 76, 444–456.

Swift, D.J.P., Phillips, S., Thorne, J.A., 1991. Sedimentation on continental margins, V. Parasequences. In: Swift, D.J.P., Oertel, G.F., Tillman, R.W., Thorne, J.A. (Eds.), Shelf Sand and Sandstones Bodies: Geometry, Facies and Sequence Stratigraphy. Spec. Publ. Int. Assoc. Sedimentol. 14, 153–187.

Thorne, J.A., Swift, D.J.P., 1991. Sedimentation on continental margins, VI. A regime model for depositional sequences, their component systems tracts, and bounding surfaces. In: Swift, D.J.P., Oertel, G.F., Tillman, R.W., Thorne, J.A. (Eds.), Shelf Sand and Sandstones Bodies: Geometry, Facies and Sequence Stratigraphy. Spec. Publ. Int. Assoc. Sedimentol. 14, 189–255.

Tornquist, T.E., 1994. Middle and Late Holocene avulsion history of the River Rhine (Rhine–Meuse delta, Netherlands). Geology 22, 714–717.

Vail, P.R., Mitchum, R.M., Thompson, S., 1977. Seismic stratigraphy and global changes of sea level, Part 3. Relative changes of sea level from coastal onlap. In: Payton, C.E. (Ed.), Seismic Stratigraphy — Applications in Hydrocarbon Exploration. Am. Assoc. Pet. Geol. Mem. 26, 63–82.

Van de Plassche, O., Roep, Th.B., 1989. Sea-level changes in the Netherlands during the last 6500 years: basal peats vs. coastal barrier data. In: Scott, D.B., Pirazolli, P.A., Honig, C.A. (Eds.), Late Quaternary Sea-Level Correlation and Applications. NATO ASI Ser., Kluwer, Dordrecht, pp. 41–56.

Vanderburgh, S., Smith, D.G., 1988. Slave River delta. Geomorphology, sedimentology and Holocene reconstruction. Can. J. Earth Sci. 25, 1990–1999.

Verdaguer, A., 1983. La plataforma continental silícico-clástica del Ebro, Mediterráneo Nor-Occidental. Un modelo sedimentario. Doctoral Thesis, University of Barcelona, 422 pp. (unpublished).

Warne, A.G., Stanley, D.J., 1995. Sea-level change as a critical factor in development of basin margins sequences: new evidence from the Late Quaternary record. In: Finkl, C.W., Jr. (Ed.), Holocene Cycles: Climate, Sea Levels and Sedimentation. J. Coastal Res. 17, 231–240.

Williams, H.F.L., Roberts, M.C., 1989. Holocene sea-level change and delta growth: Fraser River delta, British Columbia. Can. J. Earth Sci. 26, 1657–1666.

Wright, C.D., 1985. River deltas. In: Coastal Sedimentary Environments. Springer Verlag, New York, pp. 1–76.
Zazo, C., Goy, J.L., Somoza, L., Dabrio, C.J., Belluomini, G., Improta, S., Lario, J., Bardaji, T., Silva, P.G., 1994. Holocene sequence of sea-level fluctuations in relation to climatic trends in the Atlantic–Mediterranean linkage coast. J. Coastal Res. 10, 933–945.